Theory and Building Practice

Vol. 6, No.2, 2022

DOI

Maksym Koval

DETERMINATION OF BRIDGE BEAMS SERVICEABILITY USING NON-DESTRUCTIVE TESTING METHODS AND FIELD TESTS

Department of Highways and Bridges,
Lviv Polytechnic National University
maksym.p.koval@lpnu.ua

The case of determining the serviceability of bridge beams with manufacturing defects is considered. Based on the results of visual inspection and non-destructive testing, it was found that the defects have a minor impact on the performance of the beams, and the characteristics of the building materials are high. The results of the calculations showed that the beams had almost twice the safety margin compared to the design requirements. The results of field tests of beams showed reliable anchoring of the working reinforcement, proper deformability and crack resistance of the beams. Usage of the acoustic emission method during field tests allowed to establish that the beams had no internal defects that could develop under load and reduce performance. Based on the results of the research, it was concluded that the beams manufactured with defects are suitable for use after the defects have been repaired.

Keywords: acoustic emission, bridge beam, field tests, non-destructive testing, serviceability, static load

Introduction

During the reconstruction of the M-06 Kyiv - Chop highway on the section km 129+600 - 151+730 (bypassing Zhytomyr), the reconstruction project included the construction of new bridges and reconstruction of old bridges using prestressed reinforced concrete bridge beams. Construction contractor that was reconstructing mentioned section of the M-06 highway decided to produce bridge beams on its own, and for this purpose its own formwork station and formwork panels were manufactured. About a hundred prestressed reinforced concrete bridge I-beams of two types – B.1200.60.110 and B.1800.60.110 (Fig. 1) – were manufactured at this station.

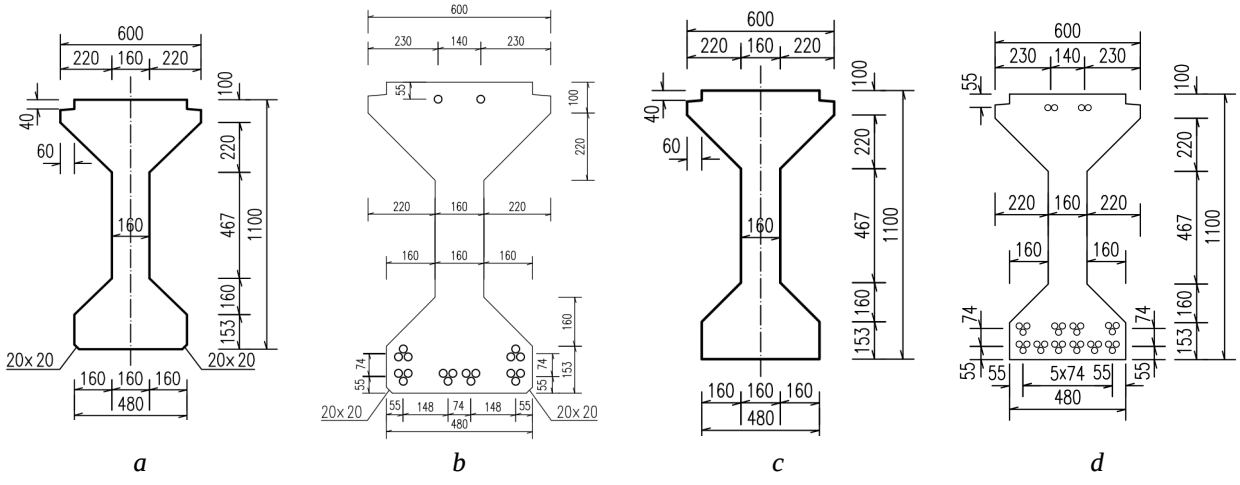

Fig. 1. Cross-sectional view:
a – and main reinforcement scheme; b – of beam type B.1200.60.110;
cross-sectional view; c – and main reinforcement scheme; d – of beam type B.1800.60.110

According to the project, both types of I-beams should be made using concrete C40/50 W8 F300. Beams B.1200.60.110 were reinforced with eighteen K-7 Ø12.7 mm seven-wire strands in the bottom flange, and the top flange were reinforced with two K-7 Ø12.7 mm seven-wire strands. Beams B.1800.60.110 were reinforced with thirty K-7 Ø12,7 mm in the bottom flange, and the top flange were reinforced with four K-7 Ø12.7 mm seven-wire strands.

The formwork was made by insufficiently qualified contractors, and the quality of the work was poor. During the electric welding process, the relatively thin metal sheets of the formwork experienced uneven temperature deformations and became wavy. The design of the side formwork panels was generally imperfect, which resulted in installation of panels with slight deviations from the vertical. This led to a slight reduction in the thickness of the beam webs and the width of their top flanges. This also led to a reduction in the protective layer of concrete for the rods of distribution reinforcement located in the webs of the beams. The imperfect design of the end formwork panels required sealing the holes in these panels, which was done before concreting with polyurethane foam; this foam also filled the small internal volume of the formwork around the seven-wire strands.

A number of defects were found in the B.1200.60.110 and B.1800.60.110 beams after manufacture. In this regard, the question arose of determining the serviceability of manufactured reinforced concrete beams for bridge construction.

Materials and Methods

The determination of reinforced concrete beams B.1200.60.110 and B.1800.60.110 serviceability began with a visual inspection (DBN V.2.3-6-2009) and measurement of the geometric dimensions of the beams, including their cross-sections.

Control concrete samples were tested using a laboratory hydraulic press (DSTU B V.2.7-214:2009). The surface strength of the beam concrete (Gehlot, Sankhla & Gupta, 2016) was measured by elastic rebound method using a "Novotest MSh-225" Schmidt hammer (DSTU B V.2.7-220:2009). The surface strength of concrete and concrete density of the beams (Gehlot, Sankhla & Gehlot, 2016) were monitored by the ultrasonic method (DSTU B V.2.7-226:2009) using an ultrasonic device "Novotest IPSM". The thickness of the concrete protective layer of the main and distribution reinforcement of the beams was determined by the magnetic method (DSTU B V.2.6-4-95) using the "Novotest Armaturoskop" device. The individual wires of the seven-wire strands were tested using a laboratory tensile testing machine.

The bearing capacity of the beams was calculated at the construction stage (when the beams operate separately) and at the operation stage (with the inclusion of all beams in the spatial operation of the span structure together with the monolithic deck slab) using the limit state method (DBN V.2.3-14:2006). The values of the beam bearing capacity were compared with the design values of the forces arising in the span structures of the designed bridges from permanent and temporary loads (DBN V.1.2-15:2009); design values were determined in the design documentation using the finite element method.

It is possible to confidently assess the serviceability of beams by obtaining scientific data on the stress-strain state of beams (Elrakib & Arafa, 2012), the nature of their operation under load, and the presence or absence of internal defects that tend to develop under load (Luchko, 2020). For this purpose, it was decided to conduct field tests of two randomly selected reinforced concrete beams B.1200.60.110 named "B-1" and "B-2". Due to the lack of a stationary test bench, an improvised field test bench (Fig. 2) was prepared, consisting of two reinforced concrete prestressed plates type VTP-21 with a height of 0.6 m. Plates VTP-21, installed on compacted soil, served as bearing surfaces on which rubber reinforced bearings and two B.1200.60.110 beams were installed.

The test load consisted of B.1200.60.110 beams stored nearby (hereinafter referred to as "ballast beams") with a mass/weight of 10,8 T = 106 kN each, which were installed on the two tested beams (Fig. 3). 14 beams were installed with a spacing of 0.65 m; in the middle a free area with a distance of 1.3 m in the beam axes was provided to create a pure bending zone. The maximum bending moment achieved during field tests is M_{14max} = 1150,1 kNm, corresponding to 82,7 % of the bending moment that occurs in the

elements of the span structure under the influence of permanent and temporary loads. The maximum transverse force achieved during the field tests is Q_{14max} = 371,0 kN, which is 63,7 % of the transverse force that occurs in the elements of the span structure under the influence of permanent and temporary loads. These levels of bending moment and transverse force roughly correspond to the actual forces encountered in beams during the operation of span structures.

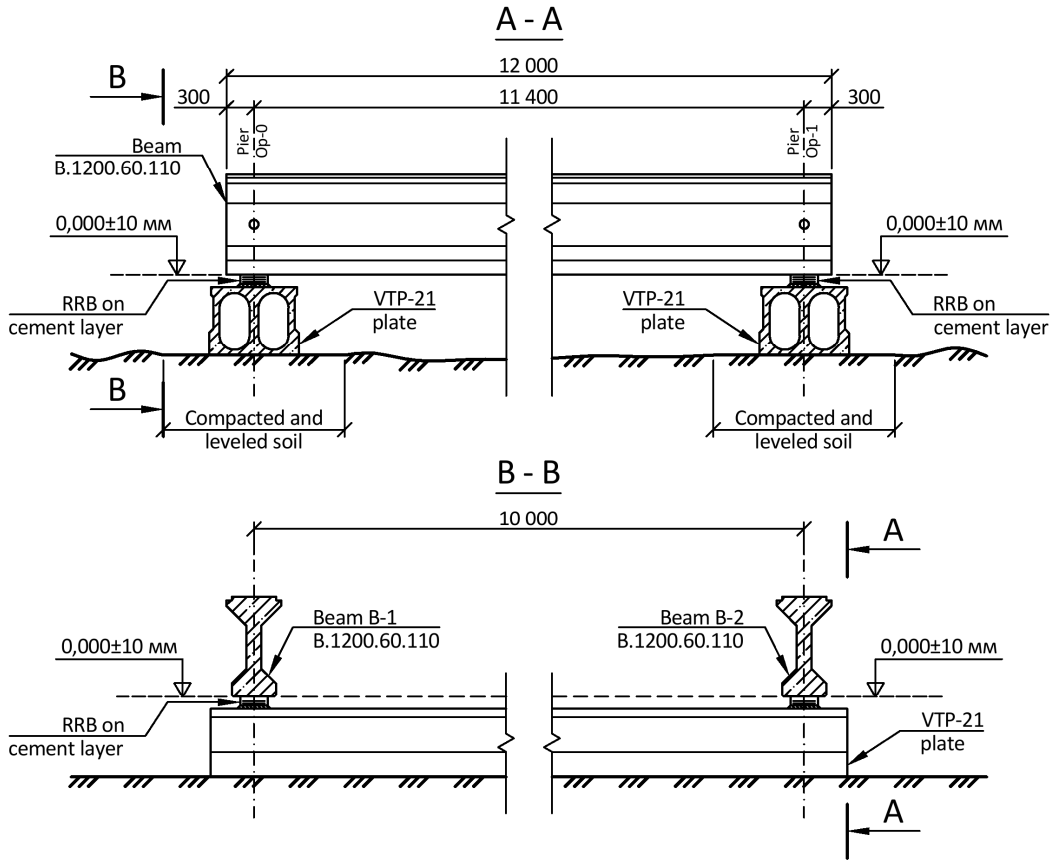

Fig. 2. The scheme of the improvised field test bench

The test program included three stages of testing, which differed in the type of static load applied to the tested beams:

1. Loading of the tested beams. During this stage, the two test beams were loaded step by step by sequential installation of ballast beams (Fig. 4).

2. Twelve-hour exposure of the tested beams under quasi-constant static load. Upon completion of the loading of the tested beams, fourteen ballast beams were left in the designated positions (Fig. 3) for 12 hours.

3. Unloading of the tested beams. After twelve hours of exposure to quasi-constant static load, tested beams were unloaded step by step by removing the ballast beams in the reverse order to the loading (from the bearing zones to the middle of the span).

The naming of the test schemes is alphanumeric: for loading - "n1", "n2" ... "n14", for unloading - "p14", "p13" ... "p0". The indexes "n" and "p" indicate loading and unloading respectively, and the scheme number corresponds to the number of ballast beams installed on the tested beams.

During the test the level of main reinforcement anchoring in the body of the beams was determined using dial gauges, the measuring heads of which were resting on the ends of the seven-wire strands. Deflections in the middle of the beam span were measured using 6PAO deflectometers; additionally, strains in the top and bottom flanges of the beams were determined using dial gauges. The absence of subsidence of the VTP-21 plates under load was monitored by the N-05 geodetic level. To obtain field

data on the presence or absence of internal defects in the beams and to assess the degree of danger of the detected defects, the acoustic emission method (Filonenko, 1999; Pullin, Holford & Lark, 2008) implemented by the software and hardware complex "AkEm" (Stakhova, 2015) was used.

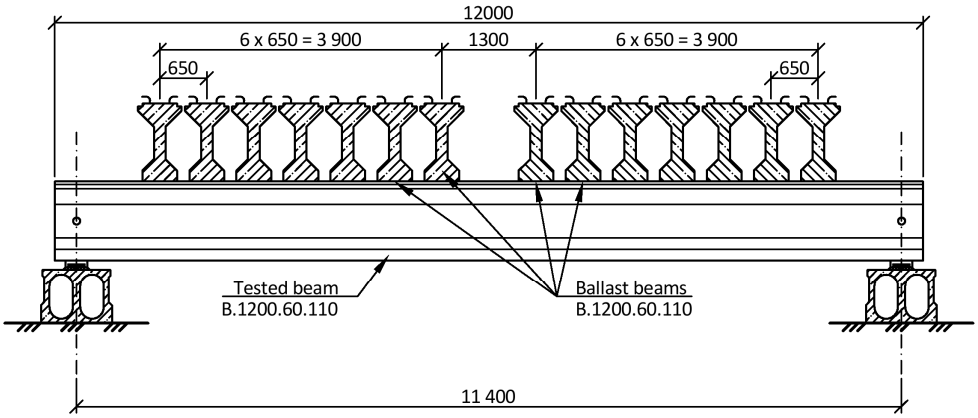

Fig. 3 – The layout of ballast beams on the tested beams

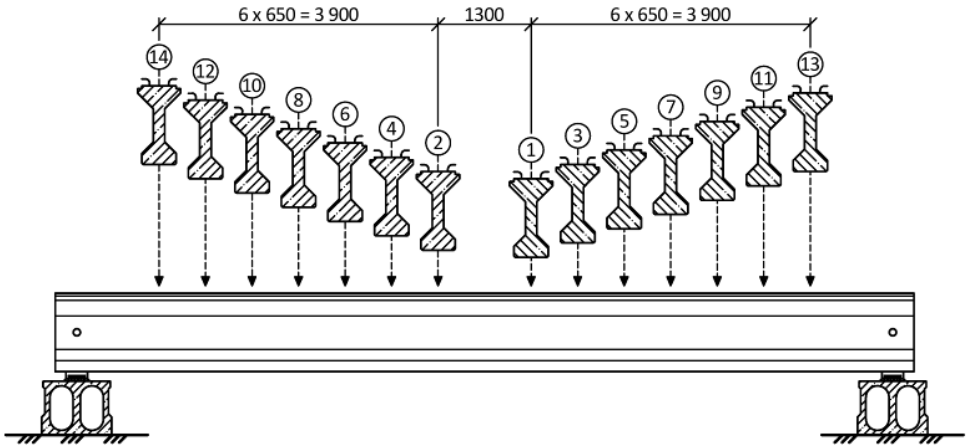

Fig. 4 – Scheme of tested beams loading sequence

The purpose of applying the acoustic emission method was to identify sources of acoustic emission (AE) that may be associated with defects that are active under loading of reinforced concrete structures; to identify the regularities of the AE process; to determine the acoustic-emission parameters of the tested beams under increasing static load (Skalskyi & Koval, 2005). Acoustic emission is the emission of elastic waves by material caused by a local, dynamic restructuring of its structure: in a certain area of a solid body local stresses reach their limit values, resulting in the destruction (fracture) of the crystal lattice (Stashuk, 2003). During this destruction (fracture), part of the elastic potential energy is released, and an elastic wave is emitted (Rucka, Knak & Nitka, 2023). An acoustic-emission sensor of high sensitivity perceives these elastic waves, converting sound vibrations into a variable voltage, and transmits it to a computer through an analog-to-digital converter for display on a monitor and storage on a hard disk (Stakhova, 2015). AE provides direct information about the development of a defect that affects structural strength and durability. At the same time, defects that do not change their parameters under increasing load, do not exhibit acoustic activity, or do not show tendencies for progressive development can be attributed to structural features. The AE method is well studied and is used in laboratory studies of materials (Aggelis, 2011), building structures (Kovalchyk, 2015; Hrymak, 2019), in testing bridge beams (Koval & Stoyanovich, 2010; Elbatanouny, Henderson & Ai, 2024), bridge span structures (MVV

218-03450778-240-2004; Li, Zhao & Kang, 2024), and in testing under different loads (Radhika & Kishen, 2024).

The primary processing of the detected AE signals from defects (e.g., cracks) was performed using the K_p coefficient. According to the theoretical provisions, the K_p parameter characterizes the degree of change in the energy density in the recorded AE signal and is used to detect signals from cracks. To determine it, the formula is used:

$$K_{pj} = \lg\left(\frac{E_{cj}}{\tau_j^2}\right), \quad (1)$$

where E_{cj} is the energy from the j-th registered AE signal; τ_j is the duration of the registered AE signal.

If the AE sensor is installed on the surface of reinforced concrete structures, the limit value of the K_p parameter is set to 6 (AE signals with the value of the $K_p < 6$ indicate the presence of inhomogeneities or defects at the microlevel within the tested structure, signals with the value of the $K_p \geq 6$ indicate the presence of macrodefects).

To assess the hazard of fracture processes based on the parameters of acoustic emission, a methodology based on the approaches of the thermokinetic nature of the fracture of solid bodies was used. Fracture is the thermosetting nucleation of an ensemble of microcracks, their fusion, and the growth of the resulting macrocrack. To compare and generalize the results independent of the dimensionality of the parameters, their scales are normalized to unity by expressions:

$$\overline{N}_H = f(\overline{P}), \quad (2)$$

$$\overline{E}_H = f(\overline{P}), \quad (3)$$

where $\overline{N}H = N_i / N_{i\max}$; $\overline{E}H = E_i / E_{i\max}$; $\overline{P} = P_i / P_{i\max}$; N_i, E_i – values of the accumulation of the number of signals and energy of the AE during the loading stages in the selected time interval; P_i – the value of the load on the stage; $P_{i\max}$ – maximum load value; $N_{i\max}$, $E_{i\max}$ – the maximum values of the accumulation of the number of signals and AE energy during the loading stages in the selected time interval.

The analysis with the approximation of the experimental data in accordance with the previously described is performed using the expressions:

$$\overline{N}_H = a_1 \overline{P}^{b_1}, \quad (4)$$

$$\overline{E}_H = a_2 \overline{P}^{b_2}, \quad (5)$$

where a_1, b_1, a_2, b_2 – constants of the corresponding expressions.

Strains relaxation due to the restructuring of the internal structure of the material at a constant load value is reflected in the kinetics of AE emission. The conclusion about the hazard of the processes occurring in the structure of materials when the object is loaded is made by the absolute value of the degree b in formulas (4) and (5). Experimental studies (Stashuk, 2003) have shown that for reinforced concrete a value of $b > 3$ indicates the development of defects.

Results and discussion

According to the results of visual inspection and careful measurements of the beams, it was found that the imperfect design of the formwork led to a 20 mm reduction in the width of the top flanges (Fig. 5, a) and to a 15 mm reduction in the thickness of the beam webs. Due to the reduced geometric dimensions of the cross-section, the thickness of the concrete protective layer of the distribution reinforcement of the beam top flange became insufficient, and some reinforcing bars were affected by surface corrosion (Fig. 5, b). The polyurethane foam used to seal the formwork penetrated into the internal volume of the formwork around the seven-wire strands, resulting in small unconcreted areas at the ends of the beams in the bottom flanges (Fig. 5, c).

Testing of control concrete samples with combine usage of the elastic rebound method and ultrasonic method (Gebauer, Gutiérrez & Krüger, 2023) allowed to establish that the strength of the beam concrete corresponds to the class C50/60 ... C55/67 (which exceeded the design strength class), and in all beams the concrete had good density and homogeneity.

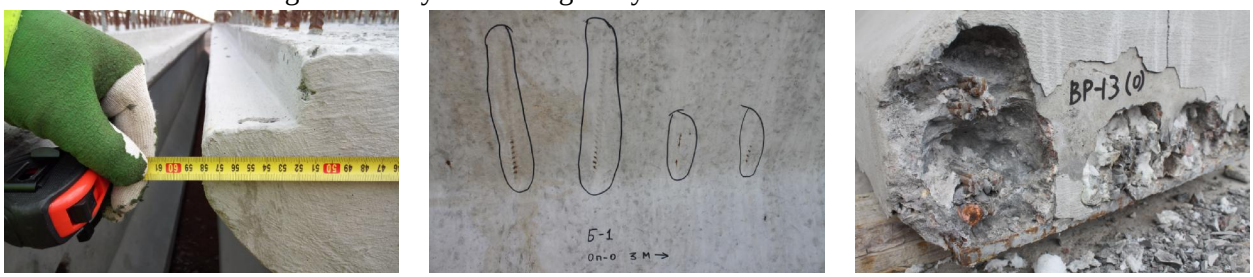

a *b* *c*

Fig. 5. Defects found in reinforced concrete beams:a– reducing the width of the upper beam belt by 20 mm; b – insufficient thickness of the concrete protective layer of the distribution reinforcement near the top flange ; c – consequences of using polyurethane foam for the formwork sealing at the end of the beam in the bottom flange

All the beams were planned to be used as statically determinated beams, and from the point of operational view the most important reinforcement is situated in bottom flange. The minimum thickness of the concrete protective layer in the bottom flanges of the studied beams, determined by the magnetic method (DSTU B V.2.6-4-95), is 52 mm for the main reinforcement and 29 mm for the distribution reinforcement; therefore, the thickness of the concrete protective layer in the bottom flanges is sufficient. It was proposed to solve the problem with the insufficient thickness of the concrete protective layer in webs and top flanges with the preservation of corroded rods by injection impregnation with a composition based on methyl methacrylate (MR V.2.3-37641918-888:2017). The unconcreted areas in the lower belts at the ends of the beams do not sustain significant stresses and could be filled with repair compounds, followed by the injection of a polymer composition based on methyl methacrylate (MR V.2.3-37641918-888:2017) to bond the repair compound to the concrete of the beam.

The results of the quality acceptance tests of the K-7 seven-wire strands showed that the strands used as prestressed main reinforcement met the passport characteristics. Additionally, axial tensile tests of individual wires were performed (Fig. 6), and it was found that the average tensile strength of steel of individual wires of K-7 strands is 3130 MPa.

The results described above allowed to conclude that the quality of concrete and main reinforcement of B.1200.60.110 and B.1800.60.110 beams is adequate. It was decided to carry out verification calculations taking into account the defective geometry of the cross-sections. Two types of beam cross-sections were compared in the calculations: design cross-sections (Fig. 1) and cross-sections with reduced geometric characteristics, which had a web thickness of 130 mm and a top flange width of 560 mm. Such a significant decrease in geometric characteristics was not observed during the inspections, but was accepted theoretically as an extreme case within the risk-based approach.

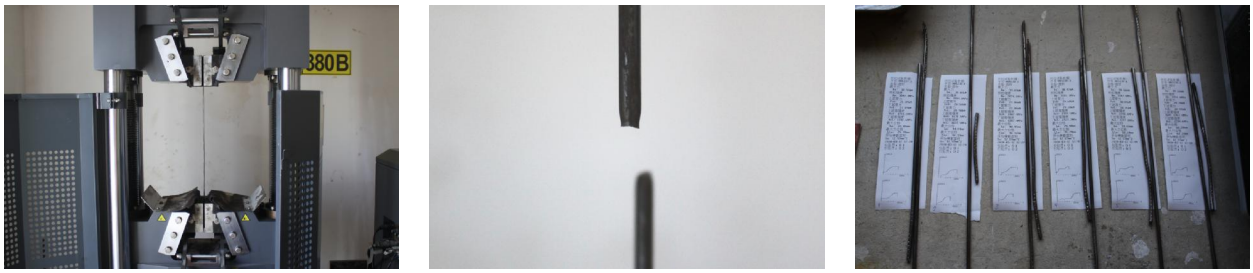

a *b* *c*

Fig. 6. Axial tensile testing of individual wires of K-7 strands: a – wire in the tensile machine ; b – view of the torn wire; c – view of a series of torn wires with test reports

The results of the calculations indicate a slight decrease in the bending moment bearing capacity of the beams at the construction stage - up to 1,63 %; at the operational stage bearing capacity of the beams will not decrease due to the appearance of a compressed zone in the monolithic deck slab above the beams. The reduction in lateral force bearing capacity for both types of beams will reach 18.75 % at both stages. However, the bending moments that will occur in the beams at the operational stage from permanent and temporary loads will amount to 48,04 %...49,40 % of the beams bearing capacity, and the transverse forces will amount to 53,74 % of the beams bearing capacity (considering the reduced cross-sectional geometry). The conclusion was made that beams had a sufficient safety margin even with the defective cross-sectional geometry. Initial conclusions were made about the suitability of the beams for bridge construction after the repair of the existing defects.

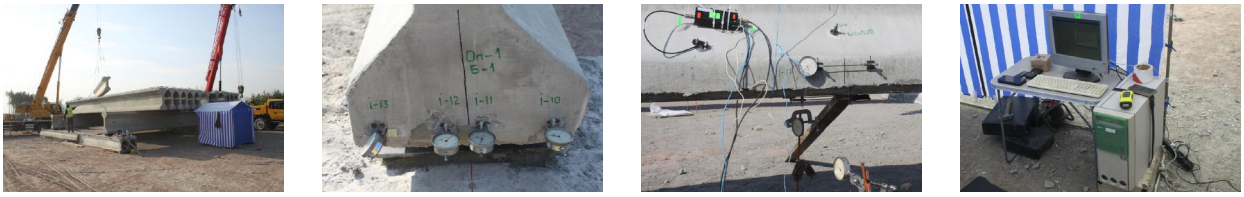

a *b* *c* *d*

Fig. 7. General view of the test bench (a); dial gauges mounted on the end of the B-1 beam (b); 6PAO deflectometers, dial gauge, AE sensor and AE amplifier installed in the middle of the B-2 beam span (c); software and hardware complex "AkEm"(d)

Field tests of two reinforced concrete beams B.1200.60.110 (Fig. 7) allowed to obtain objective data on their stress-strain state during a stepwise increase in static load, as well as during a stepwise decrease in static load after twelve hours of exposure to load.

The twelve-hour exposure of the tested beams to a quasi-constant static load was an extreme case of loading: the tested beams were not designed to withstand such a high level of constant loads for a long time. This loading scheme was designed to assess the crack resistance of beams and the effectiveness of reinforced concrete prestressing. The results indicate that the prestressing was created effectively and the crack resistance of the beams was ensured: after twelve hours of exposure, no cracks were found in the beams.

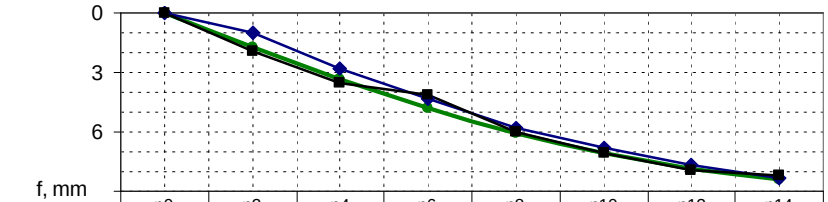

	n0	n2	n4	n6	n8	n10	n12	n14
fteor	0	1,7	3,3	4,77	6,04	7,08	7,88	8,39
fexp B-1	0,00	1,00	2,78	4,35	5,79	6,78	7,64	8,35
k B-1	0,00	0,59	0,84	0,91	0,96	0,96	0,97	0,99
fexp B-2	0,00	1,92	3,57	4,12	5,98	7,10	7,95	8,19
k B-2	0,00	1,13	1,08	0,86	0,99	1,00	1,01	0,98

Fig. 8. Graphs of f_{teor} – theoretical deflection, $f_{exp\ B\text{-}1}$ and $f_{exp\ B\text{-}2}$ – experimentally obtained deflections of beams, $k = f_{exp}/f_{teor}$ – values of constructive coefficient

The analysis of the deflections of the tested beams measured with 6PAO deflectometers (Fig. 7, c) and the comparison of these values with the deflections calculated using a finite element model with the real cross-sectional geometry indicates that the beams worked elastically during the tests (Fig. 8). The slight unevenness of beam deflections at the initial stages of loading disappears after the "n6" scheme, when the tested beams became well connected by ballast beams. The constructive coefficient *k*, calculated as the ratio of experimentally obtained deflections to theoretical deflections, is generally within

acceptable limits: after the "n6" scheme it is in the range of 0,96...1,01, which indicates normal operation of the beams in bending, sufficient cross-section stiffness and proper deformability.

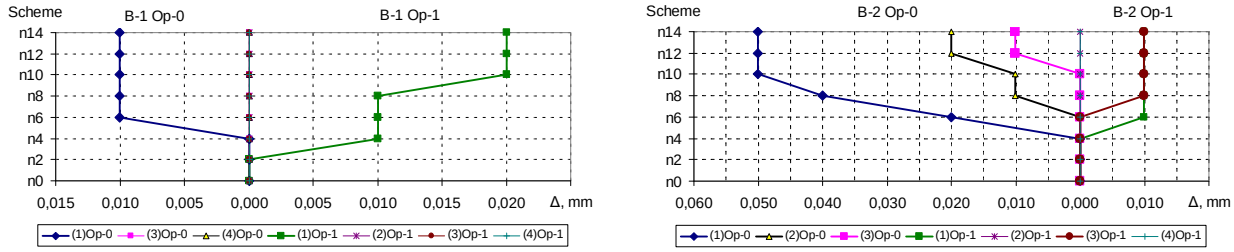

a *b*

Fig. 9. Displacement of the ends of the groups of seven-wire strands at the ends of the beams B-1 (a) and B-2 (b)

Analysis of the values of displacements of the group of seven-wire strands ends in the studied beams, measured using dial gauges with a division price of 0,01 mm (Fig. 7, b), shows that the values of these displacements are insignificant. For example, in beam B-1 during the tests displacement was recorded in only one group of strands with maximum value of 0.02 mm; in beam B-2 the displacement was recorded in three groups of strands with maximum value of 0.05 mm. The values of these displacements (Fig. 9) are very small, which indicates that the seven-wire strands was anchored securely in the concrete of the beams.

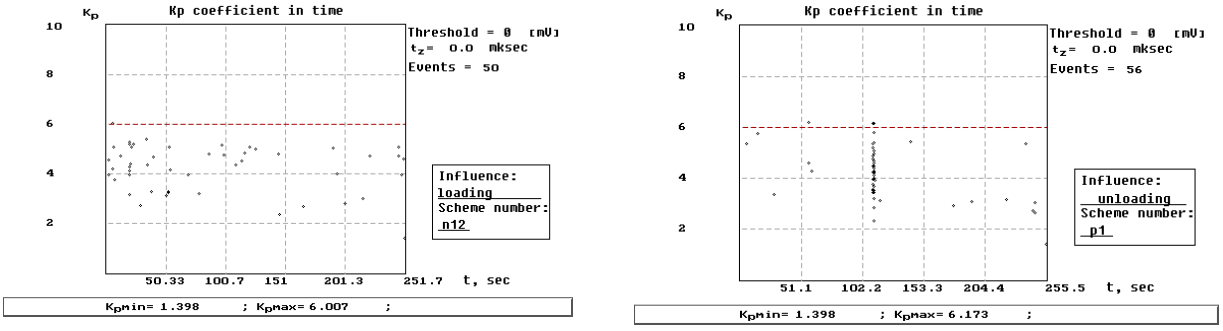

a *b*

Fig. 10. Change in the time of the coefficient K_p in scheme "n12" (a) and scheme "p1" (b)

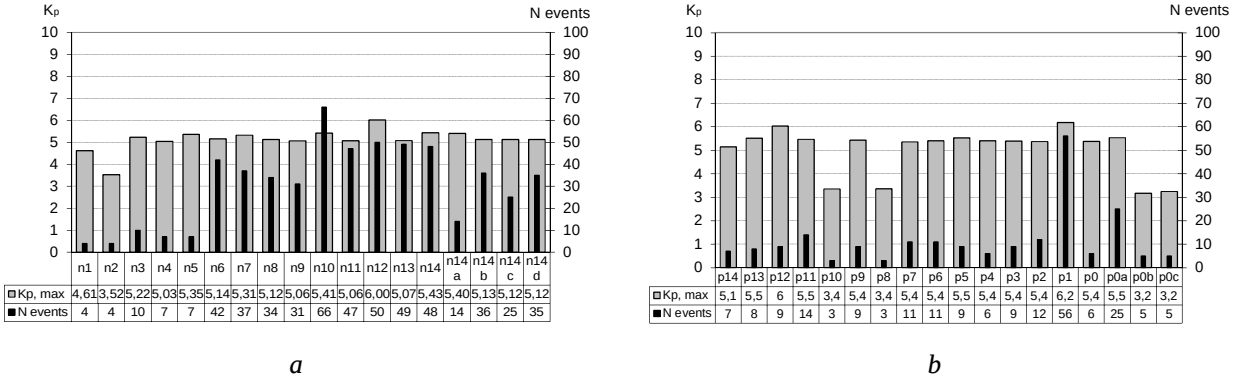

a *b*

Fig. 11. Number of events (AE signals) and maximum values of K_p coefficients at loading (a) and unloading (b) of the tested beams

The AE signals in the beam B-2 (Fig. 7, c) were recorded and analyzed upon reaching each new load level (after installing each ballast beam during loading and removing each ballast beam during unloading). The analysis of the obtained results shows that during the tests weak and single signals of acoustic emission from internal inhomogeneities (at the microlevel) were recorded. During the loading of the beams, a single signal with K_p = 6,007 was recorded at the beginning of the "n12" scheme (Fig. 10, a), but the nature of this event does not allow to classify it as a signal from a macrocrack. When the beams

were unloaded, a signal with K_p = 6,173 was recorded under the "p1" scheme (Fig. 10, b). This is a signal from a macrocrack, but it is highly likely that this signal was emitted by one of the shrinkage cracks in the top flange of the tested beam, which does not affect structural safety, and this defect does not have a tendency for dangerous development.

During other loading (Fig. 11, a) and unloading (Fig. 11, b) schemes, the maximum value of the K_p coefficient was less than 6, which indicates the absence of macrodefects in the beam structure.

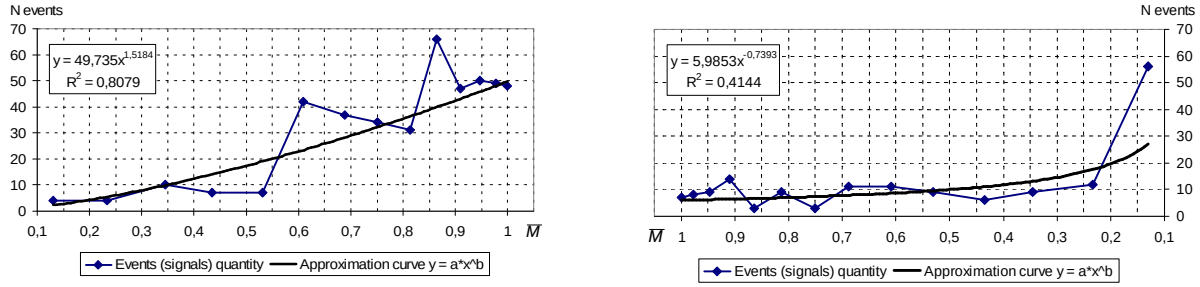

a *b*

Fig. 12. Thermokinetic estimation of AE signals quantity accumulation during loading (a) and unloading (b) of the tested beams

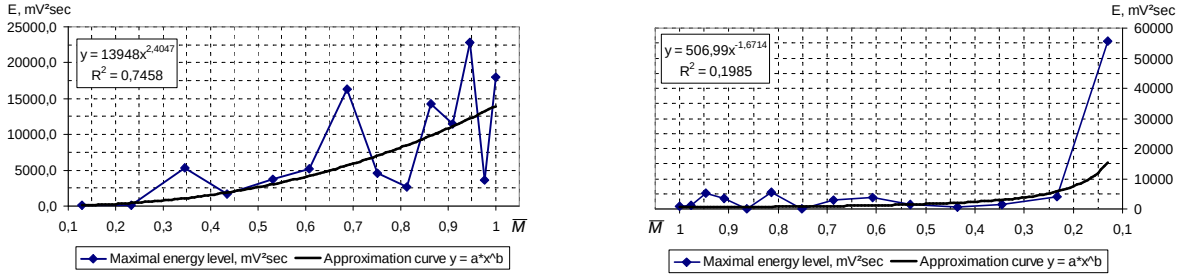

a *b*

Fig. 13. Thermokinetic estimation of AE signals energy (mV²sec) accumulation during loading (a) and unloading (b) of the tested beams

Thermokinetic evaluation of the accumulation of the signals quantity N during loading (Fig. 12, a) and unloading (Fig. 12, b) of the beams was performed using two-coordinate graphs "$\overline{M} = M_i / M_{i\max}$ – N", approximated by power polynomials of the form $y = a \times x^b$. The results of the approximation of the quantitative characteristics of AE signals indicate the absence of tendencies to defects development: during the loading of the beams, the exponent of the function is b = 1,5184 < 3; during the unloading of the beams, the exponent of the function is |b| = 0,7393 < 3.

Thermokinetic evaluation of the accumulation of the signals energy E during loading (Fig. 13, a) and unloading (Fig. 13, b) of the beams was performed using two-coordinate graphs "$\overline{M} = M_i / M_{i\max}$ – E_{max}", approximated by power polynomials of the form $y = a \times x^b$. The results of the approximation of the energy characteristics of AE signals indicate the absence of tendencies to defects development: during the loading of the beams, the exponent of the function is b = 2,4047 < 3; during the unloading of the beams, the exponent of the function is |b| = 1,6714 < 3.

Conclusions

1. Due to manufacturing reasons, prestressed concrete bridge beams B.1200.60.110 and B.1800.60.110 were manufactured with defects – reduced cross-sectional dimensions and reduced thickness of the concrete protective layer of distribution reinforcement in the beam webs. Based on the results of the beams inspection and quality control of the materials used to make the beams, it was concluded that discovered defects had a minor impact on the exploitation characteristics of the beams.

2. Thanks to the use of high-quality construction materials, in particular, high-strength concrete, properly compacted during concreting, the main operational characteristics – strength, stiffness and deformability of B.1200.60.110 and B.1800.60.110 beams – are ensured.

3. The results of verification calculations show that the reduction of the beams cross-section slightly reduces the bearing capacity of B.1200.60.110 and B.1800.60.110 beams, but they have sufficient (almost twofold) safety margins compared to the design forces.

4. The field tests of two B.1200.60.110 beams revealed that their actual deformability corresponds to the theoretical one, the main reinforcement is reliably anchored in the beam body, and the crack resistance of the beams is ensured by the prestressed main reinforcement.

5. The results of acoustic-emission diagnostics performed during field tests of the beams show that there are no internal defects in the beams that could develop under load and reduce performance.

6. The combined usage of various methods of calculation, inspection, non-destructive testing and full-scale field testing proved the serviceability of bridge beams, manufactured with minor defects. After the defects are repaired, the beams can be used in bridge construction.

7. Additional methods of defect accounting can be used to better determine the actual properties of the beams. The results of such determination can be used in the selection of methods and techniques for repairing beam defects. However, this was not the main objective of the study conducted to determine the fundamental serviceability of beams and deserves additional coverage in a separate paper.

References

Aggelis, D. G., Kordatos, E. Z., & Matikas, T. E. (2011). Acoustic emission for fatigue damage characterization in metal plates. *Mechanics Research Communications*, 38(2), 106-110. https://doi.org/10.1016/j.mechrescom.2011.01.011

Elbatanouny, E., Henderson, A., Ai, L., & Ziehl, P. (2024, September). Condition assessment of prestressed concrete channel bridge girders using acoustic emission and data-driven methods. In *Structures* (Vol. 67, p. 107008). Elsevier. https://doi.org/10.1016/j.istruc.2024.107008

Elrakib, T. M., & Arafa, A. I. (2012). Experimental evaluation of the common defects in the execution of reinforced concrete beams under flexural loading. *HBRC Journal*, 8(1), 47-57. https://doi.org/10.1016/j.hbrcj.2012.08.006

Filonenko, S. F. (1999). *Acoustic emission. Measurement, control, diagnostics.* Kyiv: KMUGA (in Russian) https://irbis-nbuv.gov.ua/publ/REF-0000001186

Gebauer, D., Gutiérrez, R. E. B., Marx, S., Butler, M., Grahl, K., Thiel, T., ... & Krüger, M. (2023). Interrelated dataset of rebound numbers, ultrasonic pulse velocities and compressive strengths of drilled concrete cores from an existing structure and new fabricated concrete cubes. *Data in brief*, 48, 109201. https://doi.org/10.1016/j.dib.2023.109201

Gehlot, T., Sankhla, S. S., Gehlot, S. S., & Gupta, A. (2016). Study of concrete quality assessment of structural elements using ultrasonic pulse velocity test. *IOSR Journal of Mechanical and Civil Engineering*, 13 (05), 15 – 22. https://www.academia.edu/29277858/Study_of_Concrete_Quality_Assessment_of_Structural_Elements_Using_Ultrasonic_Pulse_Velocity_Test

Gehlot, T., Sankhla, S. S., & Gupta, A. (2016). Study of concrete quality assessment of structural elements using rebound hammer test. *American Journal of Engineering Research (AJER)*, 5, 192 – 198. https://www.academia.edu/27925677/Study_of_Concrete_Quality_Assessment_of_Structural_Elements_Using_Rebound_Hammer_Test

Hrymak O. Ya. (2019). *Strength, deformability and crack resistance of concrete beam structures of bridges with basalt plastic reinforcement* (Dissertation of the candidate of technical sciences). Lviv, NU "Lvivska politekhnika" " [in Ukrainian]. https://old.lpnu.ua/sites/default/files/dissertation/2019/11821/dis_hrymak_o._ya.pdf

Koval, P. M., & Stoyanovich, S. V. (2010). Researches of concrete fracture strength of the beams by type "3 BET-90" and "3 BET-120". *Science and Transport Progress*, 33, 118–121. https://doi.org/10.15802/stp2010/13185

Kovalchyk Ya. I. (2015). *Strength, crack resistance and deformability of pre-stressed beam reinforced concrete span structures of bridges* (Dissertation of the candidate of technical sciences). Kyiv: NTU (in Ukrainian). https://dspace.nau.edu.ua/bitstream/NAU/15883/1/dis.pdf

Li, S. L., Zhao, Y. Q., Kang, Z. Z., & Wang, C. (2024). Acoustic emission technology-based waveguide localization method for internal tendons damage of in-service post-tensioned prestressed hollow-core slab bridges. *Measurement*, 114919. https://doi.org/10.1016/j.measurement.2024.114919

Luchko Y. Y. (2020). *Research and testing methods of building materials and structures*. Lviv, Vydavnytstvo "Levada" [in Ukrainian]. https://repository.lnau.edu.ua/xmlui/handle/123456789/579

Pullin, R., Holford, K. M., Lark, R. J., & Eaton, M. J. (2008). Acoustic emission monitoring of bridge structures in the field and laboratory. *Journal of Acoustic Emission*, 26, 172 – 181. https://www.academia.edu/18145004/Acoustic_Emission_Monitoring_Of_Bridge_Structures_In_The_Field_And_Laboratory

Radhika, V., & Kishen, J. C. (2024). A comparative study of crack growth mechanisms in concrete through acoustic emission analysis: Monotonic versus fatigue loading. *Construction and Building Materials*, 432, 136568. https://doi.org/10.1016/j.conbuildmat.2024.136568

Rucka, M., Knak, M., & Nitka, M. (2023). A study on microcrack monitoring in concrete: discrete element method simulations of acoustic emission for non-destructive diagnostics. *Engineering Fracture Mechanics*, 293, 109718. https://doi.org/10.1016/j.engfracmech.2023.109718

Skalskyi V. R., & Koval P. M. (2005). *Acoustic emission during the destruction of materials, products and structures. Methodological aspects of information selection and processing*. Lviv, Spolom (in Ukrainian). https://nvd-nanu.org.ua/ff674970-6889-5131-9599-a684b2a7cd2c/

Stakhova A. P. (2015) System of non-destructive control by acoustic emission method for static and dynamic types of tests. *Bulletin of Engineering Academy of Ukraine*, 4, 127 – 129 (in Ukrainian). https://dspace.nau.edu.ua/bitstream/NAU/25550/1/visnyk2015.pdf

Stashuk P. M. (2003) *Improving the determination of crack resistance of reinforced concrete structures by the method of acoustic emission* (Dissertation of the candidate of technical sciences). Lviv, NU "Lvivska politekhnika" (in Ukrainian). http://195.20.96.242:5028/lvportal/DocDescription?docid=LvNULP.BibRecord.120775

М. П. Коваль
Національний університет "Львівська політехніка",
Кафедра автомобільних доріг та мостів

ВИЗНАЧЕННЯ ЕКСПЛУАТАЦІЙНОЇ ПРИДАТНОСТІ МОСТОВИХ БАЛОК ЗА ДОПОМОГОЮ МЕТОДІВ НЕРУЙНІВНОГО КОНТРОЛЮ ТА ПОЛЬОВИХ ВИПРОБУВАНЬ

У практиці будівництва трапляються випадки виготовлення залізобетонних конструкцій із виробничими дефектами. У роботі розглянутий випадок із визначенням експлуатаційної придатності мостових залізобетонних попередньо напружених балок, які були виготовлені із дефектами, породженими недосконалостями виробничого стенду. За результатами візуального обстеження та методів неруйнівного контролю було встановлено, що дефекти чинять незначний вплив на експлуатаційні характеристики балок, самі балки були виготовлені із належно ущільненого бетону високої міцності, була забезпечена належна товщина захисного шару арматури нижнього поясу балок, а робоча арматура мала належну міцність на розтяг. Результати проведених розрахунків перерізів балок із врахуванням зменшеної геометрії перерізу засвідчили, що при незначному зменшенні фактичної несної здатності балки володіли майже двократними запасами міцності порівняно із проектними зусиллями у елементах прогонових будов на стадії експлуатації. Об'єктивні дані про напружено-деформований стан виготовлених балок були отримані під час виконання польових випробувань двох балок, які були ступінчасто завантажені постійним навантаженням, піддані дванадцятигодинній витримці під навантаженням та розвантажені. Результати випробувань засвідчили про надійне анкерування робочої арматури в нижніх поясах балок, був зроблений висновок про належну деформативність та тріщиностійкість балок. Завдяки застосування методу акустичної емісії під час випробувань балок було встановлено, що у балках відсутні внутрішні дефекти, які можуть розвиватися під навантаженням та знизити експлуатаційні характеристики. За результатами проведених досліджень був зроблений висновок, що балки, виготовлені з дефектами, придатні до експлуатації після виконання робіт з ремонту дефектів.

Ключові слова: акустична емісія, польові випробування, залізобетонна балка, експлуатаційна придатність, неруйнівний контроль, статичне навантаження.